

**Conformal Coating of a Phase Change Material on Ordered Plasmonic
Nanorod Arrays for Broadband All-Optical Switching**

*Peijun Guo¹, Matthew S. Weimer^{2,3}, Jonathan D. Emery⁴, Benjamin T. Diroll¹, Xinqi Chen^{5,6}, Adam S. Hock^{2,7}, Robert P. H. Chang⁴, Alex B. F. Martinson³, Richard D. Schaller^{1, 8, *}*

¹Center for Nanoscale Materials, ³Materials Science Division and ⁷Chemical Sciences and Engineering Division, Argonne National Laboratory, 9700 South Cass Avenue, Lemont, IL 60439 USA

²Department of Chemistry, Illinois Institute of Technology, 3101 South Dearborn Street, Chicago, IL 60616 USA

⁴Department of Materials Science and Engineering, ⁵Department of Mechanical Engineering, ⁶Northwestern University's Atomic and Nanoscale Characterization Experimental Center (NUANCE) and ⁸Department of Chemistry, Northwestern University, 2145 Sheridan Road, Evanston, IL 60208 USA

*Email: schaller@anl.gov, schaller@northwestern.edu (Richard D. Schaller)

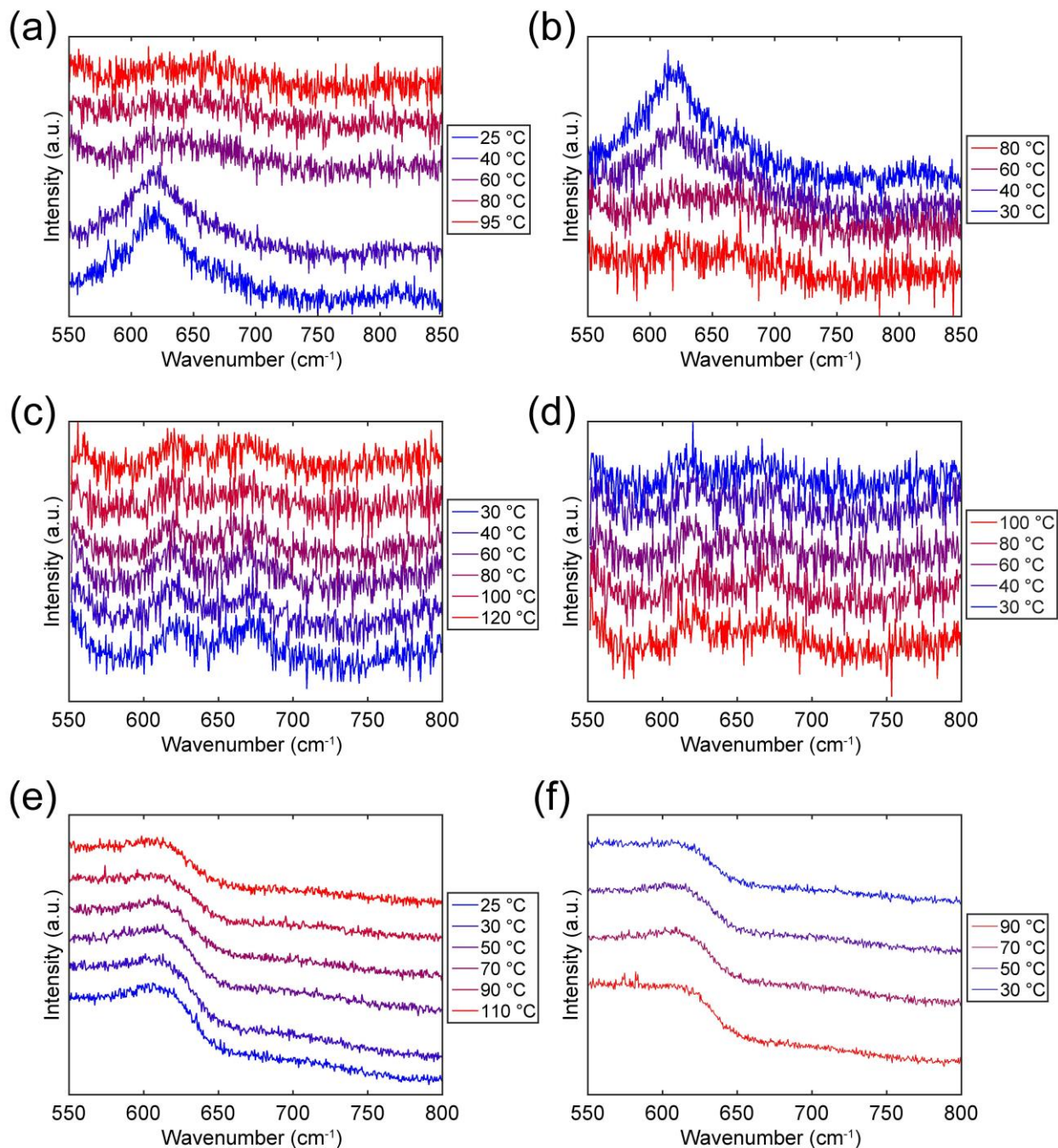


Figure S1. (a) and (b) Temperature dependent Raman spectra for VO₂ film deposited on witness Si/SiO₂ substrate (grown in the same batch with sample I). (a) was taken during heating whereas (b) was taken during cooling. (c) and (d) are same as (a) and (b) but are for a control Si/SiO₂ substrate without VO₂ coating. (e) and (f) are same as (a) and (b) but are for a control ITO-NRA sample without VO₂ coating. All curves are vertically displaced for clarity.

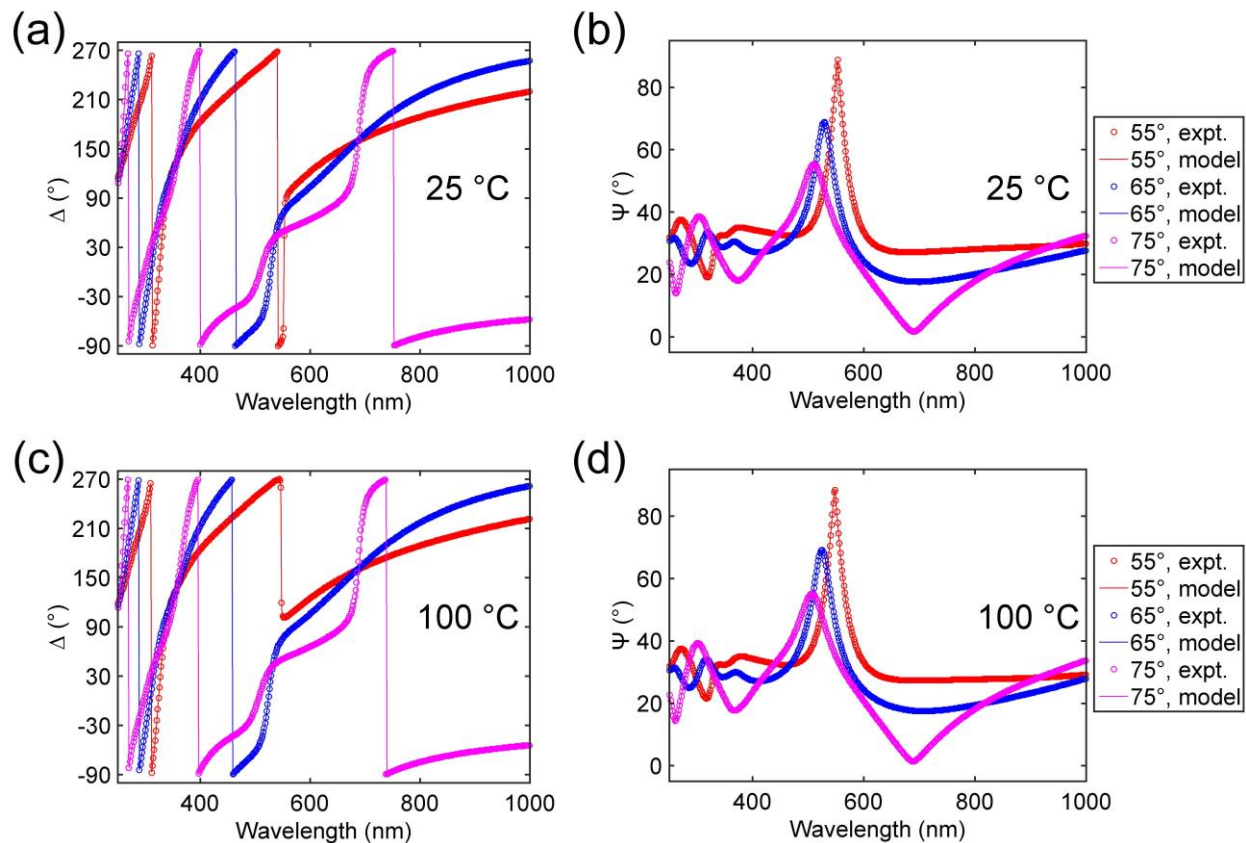


Figure S2. Δ and Ψ values for VO₂ film on witness Si/SiO₂ wafer (grown in the same batch with sample I) obtained from variable angle ellipsometric measurements performed at 25 °C shown in (a) and (b), and at 100 °C shown in (c) and (d). Fitting yielded a VO₂ thickness of 16.0 nm. The B-spline model in CompleteEASE (J.A. Woollam Co.) was used to fit the data.

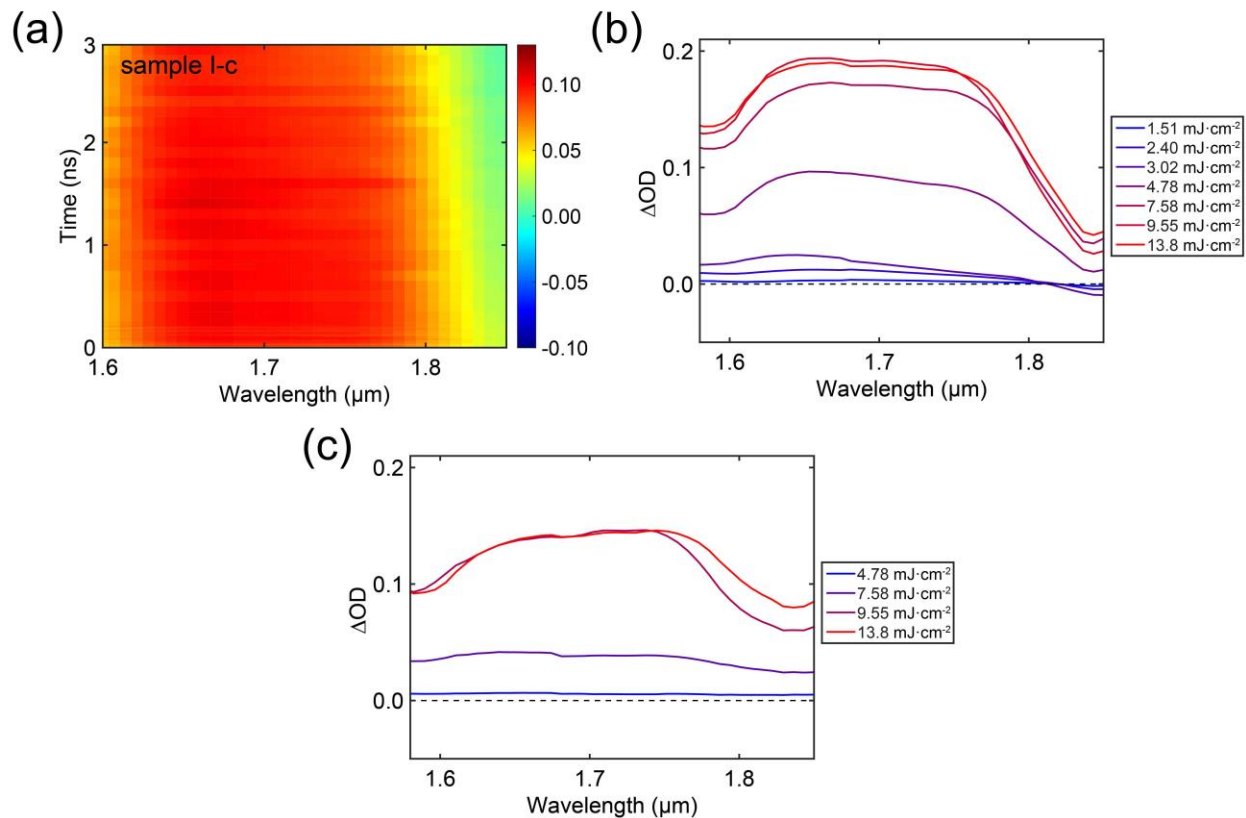


Figure S3. (a) Transient spectral map for sample I-c plotted for delay times up to 3 ns under pump wavelength of 1580 nm and fluence of $4.78 \text{ mJ}\cdot\text{cm}^{-2}$. (b) Fluence dependent transient spectra for sample I-c averaged over delay time window from 2 ns to 3 ns. (c) Fluence dependent transient spectral for sample I-film-c averaged over delay time from 2 ns to 3 ns.

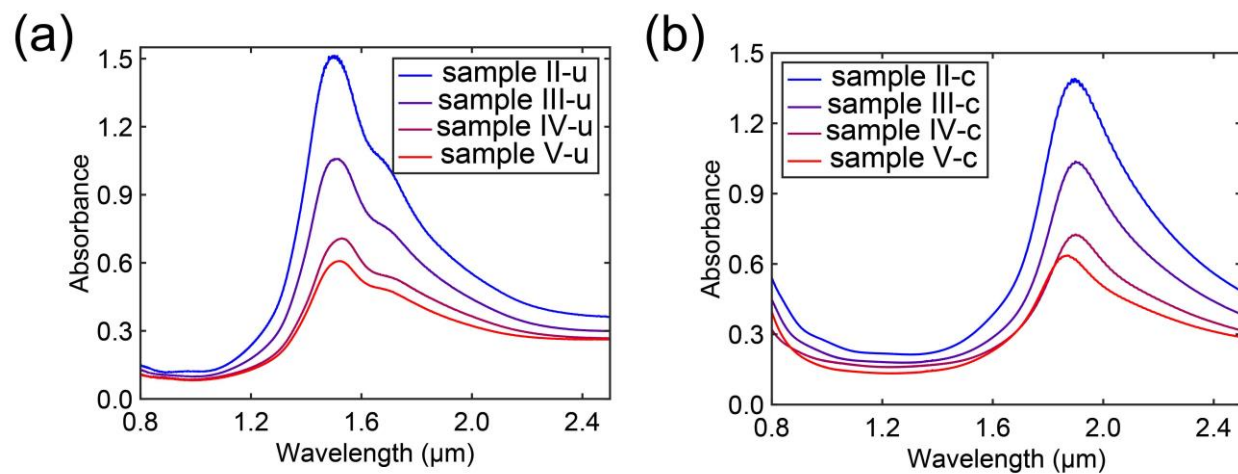


Figure S4. Near-infrared transmission spectra for sample II to sample V at normal incidence. (a) Before VO_2 coating. (b) After VO_2 coating.

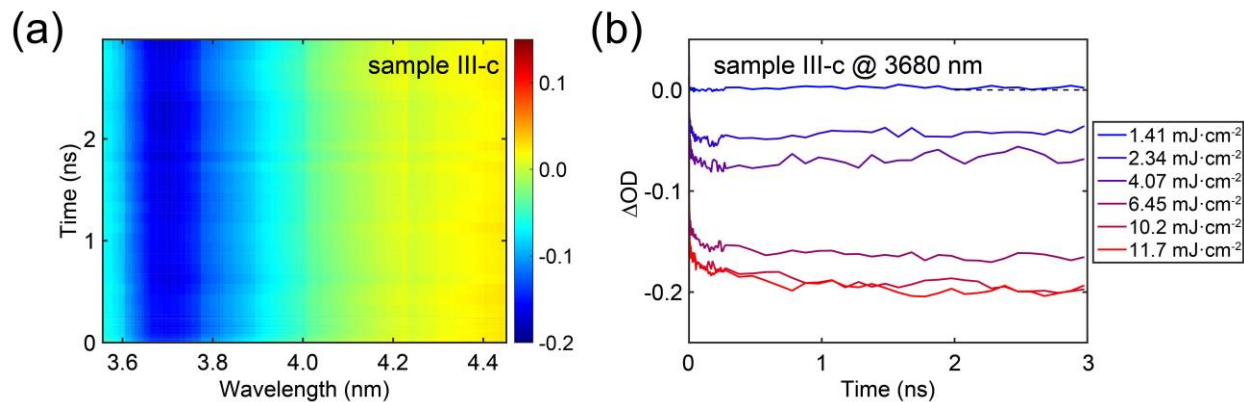


Figure S5. (a) Transient spectral map for sample III-c plotted for delay times up to 3 ns under pump wavelength of 1580 nm and fluence of 6.45 mJ·cm⁻². (b) Fluence dependent ΔOD kinetics for sample III-c at 3680 nm plotted for delay times up to 3 ns.

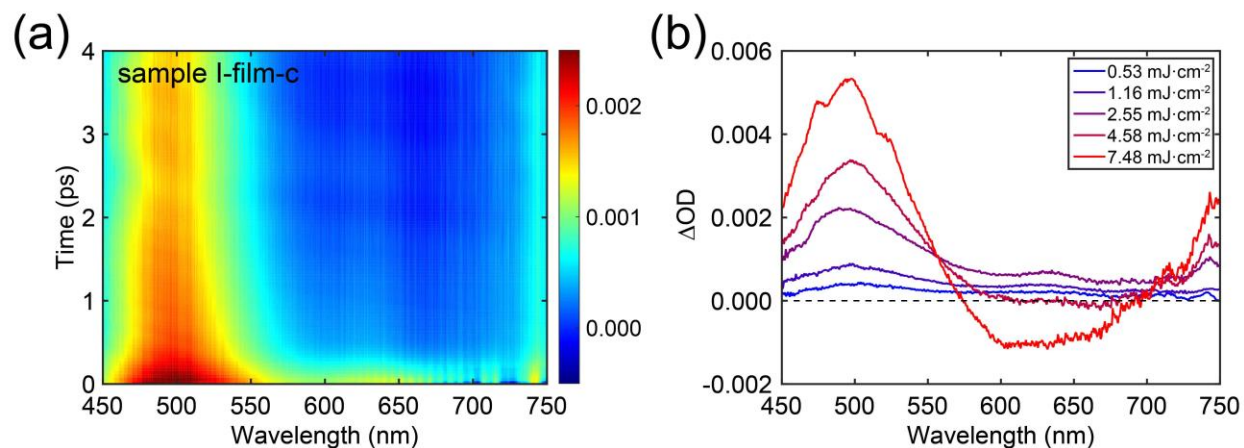


Figure S6. (a) Transient spectral map for sample I-film-c plotted for delay times up to 4 ps under pump wavelength of 1850 nm and fluence of 2.55 mJ·cm⁻². (b) Time averaged (from 2 ns to 3 ns delay time), fluence dependent transient spectra for sample I-film-c.

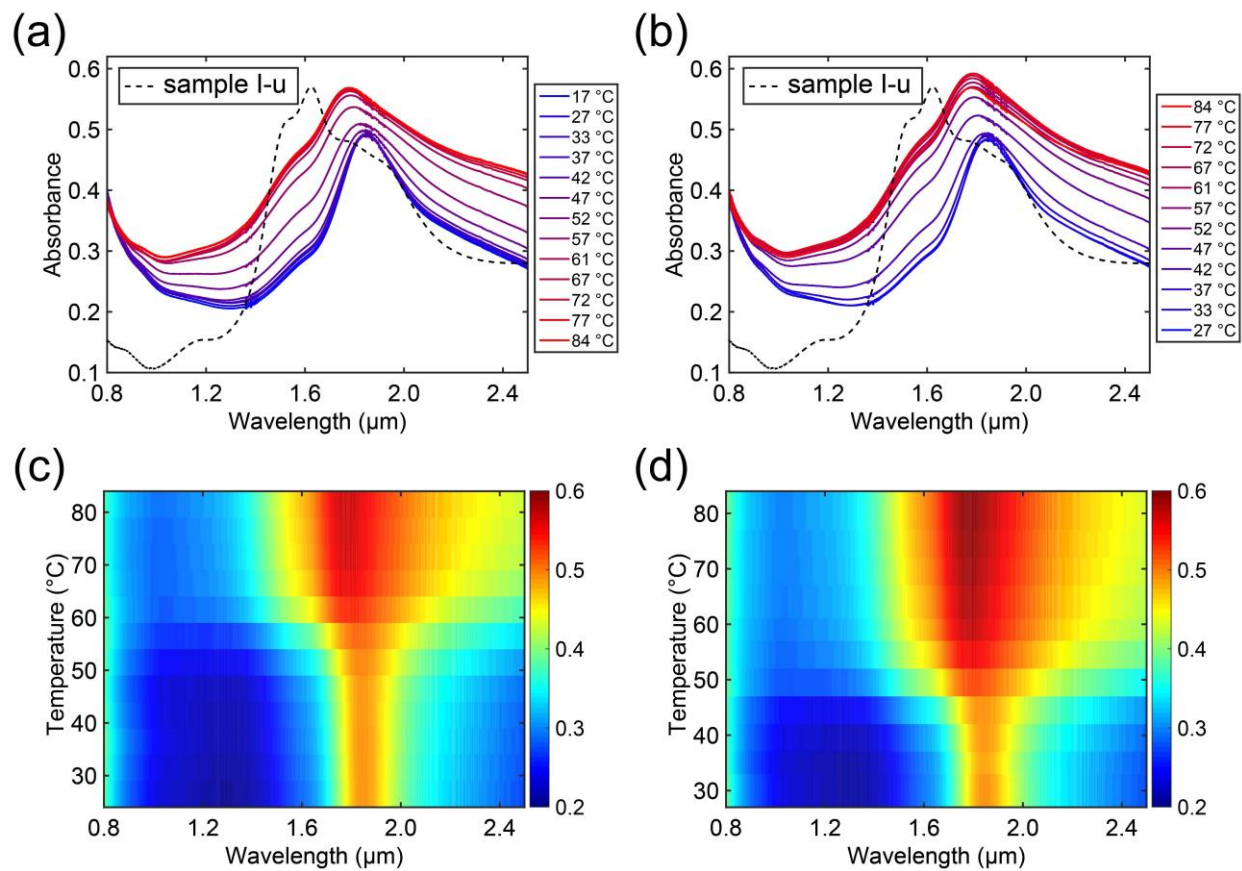


Figure S7. (a) Temperature dependent absorbance spectra for sample I-c during heating. (b) Temperature dependent absorbance spectra for sample I-c during cooling. Dashed lines in (a) and (b) are the absorbance spectra for sample I-u. (c) and (d) are color-coded versions of (a) and (b).

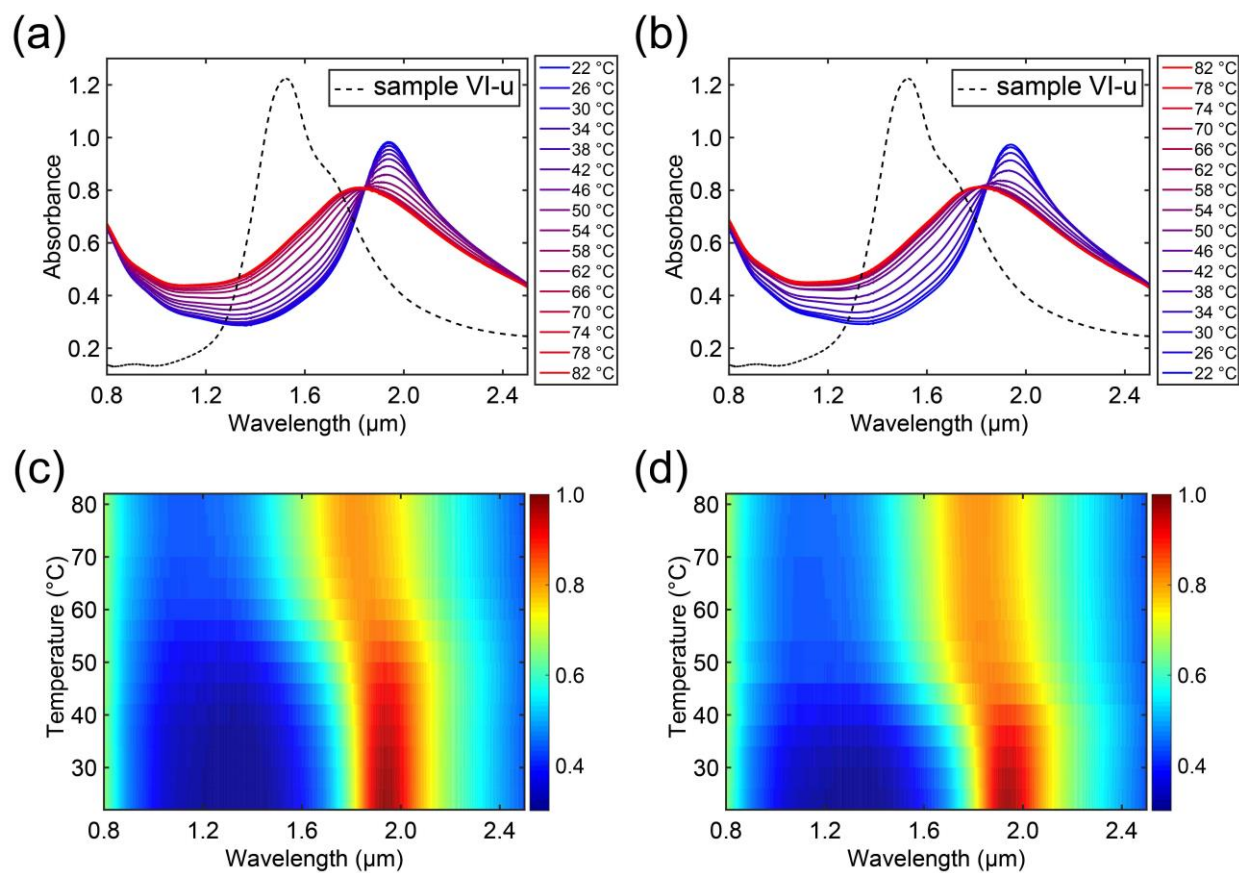


Figure S8. (a) Temperature dependent absorbance spectra for sample VI-c during heating. (b) Temperature dependent absorbance spectra for sample VI-c during cooling. Dashed lines in (a) and (b) are the absorbance spectra for sample VI-u. (c) and (d) are color-coded versions of (a) and (b).

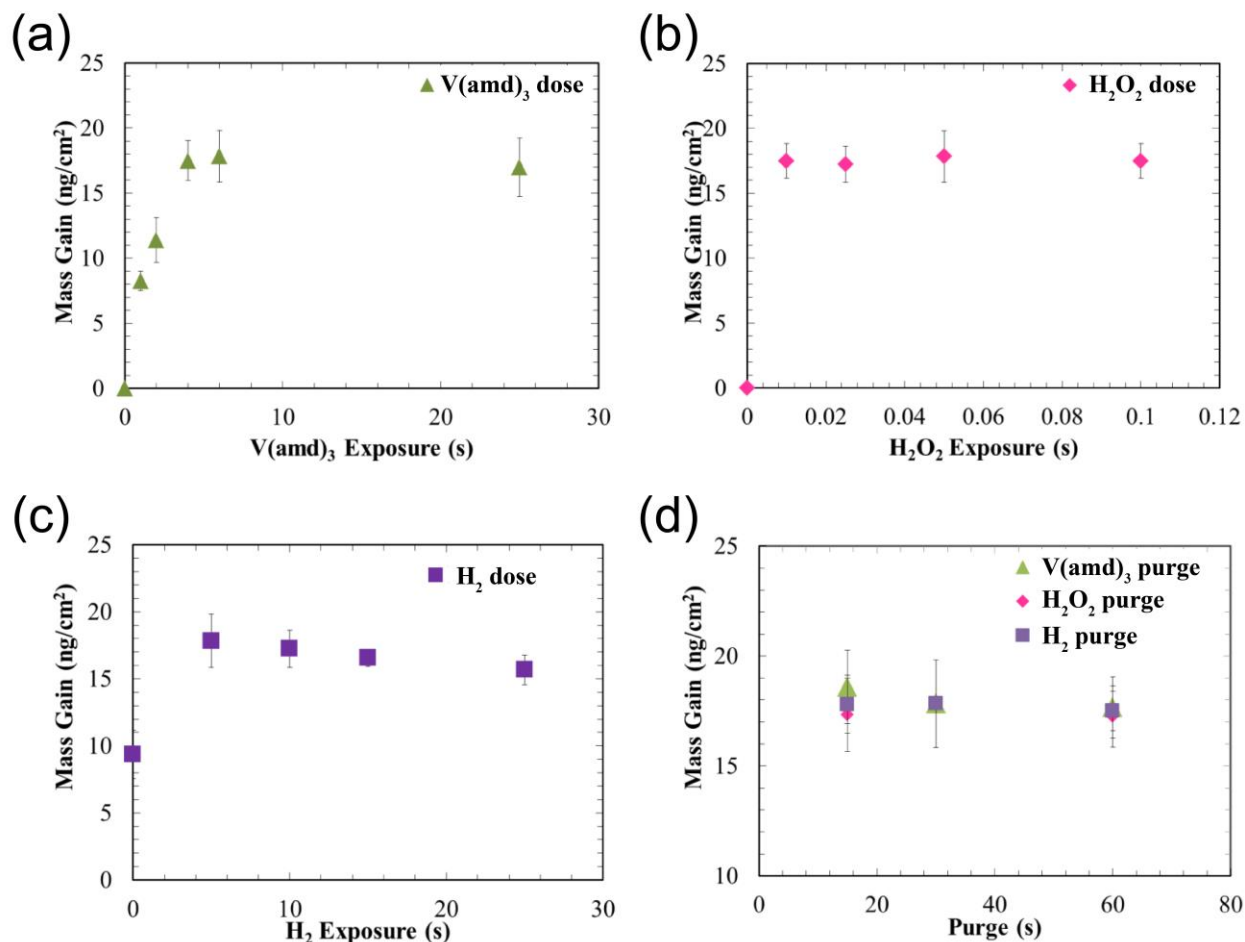


Figure S9. Plots for mass gain v.s. dose length of the V(amd)₃/H₂O₂/H₂ process at 200 °C for (a) V(amd)₃ (dose sequence follows x/30 sec/0.05 sec/20 sec/5 sec/30 sec). (b) H₂O₂ (dose sequence follows 6 sec/30 sec/x/20 sec/5 sec/30 sec). Plots for mass gain v.s. purge length of the V(amd)₃/H₂O₂/H₂ process at 200 °C for (d) V(amd)₃ (dose sequence follows 6 sec/x/0.05 sec/20 sec/5 sec/30 sec), H₂O₂ (dose sequence follows 6 sec/30 sec/0.05 sec/x/5 sec/30 sec), and H₂ (dose sequence follows 6 sec/30 sec/0.05 sec/20 sec/x). In all plots x was the variable shown in the x-axis.

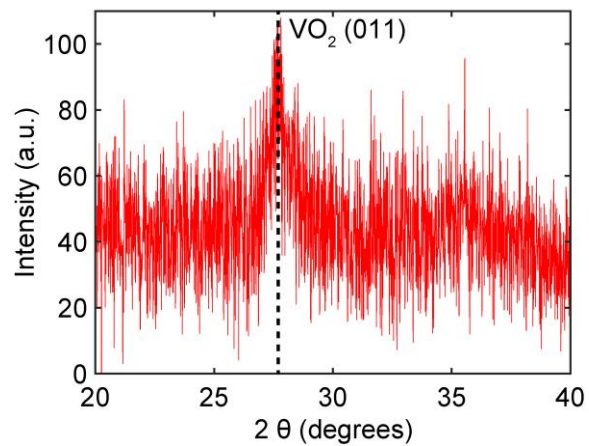


Figure S10. X-ray diffraction data (θ - 2θ scan) for VO₂ film deposited on quartz substrate. The low signal-to-noise ratio is due to the ultrathin VO₂ thickness (~ 10 nm).